EJGO European Journal of Gynaecological Oncology

Umbilical cord-derived mesenchymal stem cells efficiently induced apoptosis of endometrial carcinoma cells

J. Zheng[1*], P. Liu[2*], C. Li[1], L. Cheng[1], Y. Xu[1], F. Guo[1], M. Xiong[1], T. Song[1], Y. Li[1], F. Yan[1], H. Xu[1], B. Chen[1], J. Zhang[1]

[1]Department of Gynecology and Obstetrics, Xijing Hospital, The Fourth Military Medical University, Xi'an, Shaanxi
[2]Department of Otolaryngological, Tangdu, The Fourth Military Medical University, Xi'an, Shaanxi (China)

Summary

Purpose of Investigation: To investigate the mechanism of apoptosis of AN3CN cells, an endometrial cancer (EC) cell line, induced by human umbilical cord mesenchymal stem cells (hUCMSCs). *Materials and Methods:* UC-MSCs and AN3CN cells were co-cultured and CCK-8 cell proliferation assay was used to assess cell proliferation. *Results:* By co-culture with hUCMSCs, the proliferation of AN3CN cells was significantly inhibited ($p < 0.001$) and the cell cycle of AN3CN cells was arrested in the G2 phase. Furthermore, this study indicated that changes in the PI3K/Erk/JNK/Bcl-2/DR5 signal pathway-related genes promoted apoptosis of AN3CN cells. *Conclusion:* This finding not only helps us understand the molecular mechanism of hUCMSCs inhibiting tumor growth and promoting apoptosis, but also provides us a strong rationale to further investigate hUCMSCs as a potential treatment of EC.

Key words: Apoptosis; AN3CN cells; Human umbilical cord mesenchymal stem cells; PI3K/Erk/JNK/Bcl-2/DR5.

Introduction

Endometrial cancer (EC) is the most common female gynecological malignancy cancer, the occurrence of which has risen rapidly in Asian countries [1, 2]. The increasing incidence of EC may be related to the improvement of socioeconomic level, the incidence of obesity and metabolic syndrome, population aging, and other related factors [3]. However, there is still a lack of effective prediction, screening and early diagnosis methods for this disease. Although clinical surgery, radiotherapy, and chemotherapy have some effects, many patients suffered relapses and drug resistance.

In recent years, mesenchymal stem cells (MSCs) have demonstrated a tropism for tumors including fibrosarcoma, melanoma, renal carcinomas, hepatocellular carcinoma, breast cancer, and ovarian cancer [4, 5]. MSCs suppress tumor growth in a myriad of ways and could infiltrate the tumor stroma [6, 7]. Human umbilical cord mesenchymal stem cells (hUCMSCs) is one type of MSCs, which express genes specific to embryonic stem cells, such as SOX2, OCT4, and NANOG [8]. Compared with bone marrow mesenchymal stem cells, one of the most studied stem cells, hUCMSCs have more extensive application prospects because of the advantage of simple access, rapid self-renewal, low immunogenicity, and the absence of tumorigenicity [9]. The promising effects of hUCMSCs have been widely used in stem cells therapy [10]. In addition, hUCMSCs exhibit tumor suppressor activity on glioblastoma cancer stem cells [5], multiple myeloma [11], and other tumors. However, the antitumor mechanism of hUCMSCs in endometrial cancer cells remains unclear.

In the present study, the authors determined whether hUCMSCs can inhibit the proliferation of ECs and promote the apoptosis of ECs by paracrine pathway. The signal pathway involved in apoptosis of AN3CN cells induced by hUCMSCs was primarily investigated.

Materials and Methods

AN3CN EC cells were obtained from the American Type Culture Collection (ATCC) and maintained in DMEM containing 10% fetal bovine serum and 1% penicillin-streptomycin. AN3CN cells were cultured at 37°C with 5% CO_2. Human umbilical cords (UCs) were collected from pregnant women planning to undergo cesarean sections. All donors signed the informed consent in accordance with the ethics committee of the Xijing Hospital.

Fresh UC tissues were stored in HBSS complemented with 100 U penicillin/10.000 U streptomycin and isolated under sterile conditions. The fresh UC tissues were washed three times with HBSS to remove residual blood. The remaining tissues were diced into small fragments (1~2 mm^3), which were washed by PBS and centrifuged for ten minutes three times at 450 g at 4°C. The precipitate was digested with a mixture of 0.2 mg/ml collagenase type II and 0.25% trypsin, then the cells were collected and centrifuged at 500 g for ten minutes. The cell pellets were suspended in DMEM-F12 supplemented with 10% fetal bovine serum (FBS), 100 U/ml penicillin, and 100 U /ml streptomycin and cultured for ten days at 37°C with saturated humidity and 5% CO_2 and fed by replacing the culture medium twice weekly until confluence was observed [12].

When hUCMSCs at passage 3 reached 80% confluence, the

*Contributed equally.

Revised manuscript accepted for publication October 30, 2018

media were replaced with serum-free DMEM, and UC-MSC-CM was collected after a 24- or 48-hour incubation. The supernatants were collected and centrifuged at 1000 g for three minutes to remove cell debris.

HUCMSCs were plated at a density of 1×10^4 cells/well in 24-well plates and induced to differentiate into adipocytes with culture medium DMEM supplemented with 0.5 mM IBMX, 1uM dexamethasone and 10 μg/mL insulin. After ten days induction of differentiation, the lipids were analyzed by oil red O staining.

To investigate the osteogenic differentiation capacity of hUCMSCs, cells were cultured in 24-well plates until reaching confluence. Then the medium were replaced with osteogenic induction medium α-MEM supplemented with 10% FBS containing 10 nmol/L dexamethason, 10 mmol/L β-glycerol phosphate, 50 μg/mL ascorbic acid. After seven days, the cells were authenticated with the alkaline phosphatase staining kit. For neurogenic differentiation, hUCMSCs were cultured in DMEM/F12 supplemented with 5 μmol/L retinoic acids (RA) for 6–10 days and analyzed by anti-betaIII Tubulin staining.

To observe the effect of endogenous factors and exogenous factors secreted by hUCMSCs on AN3CN cells, the third generation of hUCMSCs and AN3CN cells were co-cultured in a Transwell system (24 mm Transwell with a 0.4-μm pore polycarbonate membrane insert). In brief, AN3CN cells were cultured in the bottom of a six-well plate at a density of 6×10^5 cells/well and hUCMSCs were seeded on the Transwell membrane at a density of 6×10^4 cells/well to separate the cells but allow soluble factors to pass freely between them.

Cell counting kit (CCK-8) was used to assess cell proliferation [13]. AN3CN cells were seeded with a concentration of 3000 per well in 96-well plates with DMEM containing 5% FBS and incubated for 24 hours. The confluent cells were cultured with DMEM containing 0.5% FBS for 12 hours for synchronization, then the medium was replaced with 0.5% FBS UC-CM-24 h or UC-CM-48 h using 0.5% FBS DMEM as control. After 24 hours, CCK-8 (10 μL/well) was added and incubated for four hours, the absorbance values of which at 450 nm were measured for five consecutive days by enzyme immunoassay analyzer.

The cells were wash twice with cold PBS then resuspended with 500 uL PBS and slowly dribbled with 5 ml cold ethanol and fixed overnight at 4°C. After centrifugation with 1,000 g for five minutes, the cells were diluted with PBS and recentrifuged twice. Cells were resuspended in 500 uL of cold PBS, added 20 uL of Ranse A and incubate in a 37°C water bath for 30 minutes. The cells were centrifuged at 1,000 g for ten minutes and then incubated with 400 μL of PI staining buffer at 4°C for 30 minutes in the dark. For co-cultured cells, AN3CN cells were digested with 0.25% trypsin without EDTA for three minutes at 37°C. Dissociated cells were washed with precooling PBS twice and 1×10^6 cells were resuspended in 400 μL1x Annexin V binding buffer. After incubation for 15 minutes at 2~8°C in the presence of 5 μL Annexin V-FITC, cells were added with 10 μL propidium iodide in binding buffer. The cell cycles were analyzed with a flow cytometer at 488 nm.

AN3CN cells were plated in six-well plates and grown until confluency. AN3CN cells were co-cultured with hUCMSCs by Transwell for 24 and 48 hours. AN3CN cells were digested with 0.25% trypsin without EDTA for three minutes at 37 °C. Dissociated cells were washed with precooling PBS twice, 4°C centrifugal 300 g, five minutes each time and collected 1×10^6 cells. Resuspended in 400 μL1x Annexin V binding buffer, and then incubated for 15 minutes at 2~8 °C in the presence of 5 μL Annexin V-FITC and then 10 μL propidium iodide for five minutes in binding buffer as described by the manufacturer, the above incubation experiment in dark conditions. After incubation, the cells were analyzed by flow cytometry.

Cells were fixed in 4% paraformaldehyde for 15 minutes and permeabilized for ten minutes with 0.5% Triton X100. Cells were then blocked with 10% normal goat serum in PBS for two hours at room temperature. Anti-human βIII-tubulin were 1:200 diluted and the secondary antibodies anti-rabbit IgG were 1:1000 diluted. Nuclei were counterstained with DAPI (1:5000) in PBS for five minutes at room temperature. The images were acquired by fluorescence microscope.

Total RNAs of AN3CN cells co-cultured with hUCMSCs for 48h were isolated using TRIzol reagent. Then, the RNA-Seq experiments were performed.

Cells were lysed in RIPA buffer containing the complete protease inhibitor mixture for ten minutes at 4°C. Nuclei were removed by centrifugation (5,000 rpm at 4°C, for ten minutes), and total protein content measured using Bradford assay. Proteins (20 mg) were resuspended in Laemmli buffer (2% SDS, 62.5 mM Tris, pH 6.8, 0.01% bromophenol blue, 1.43 mM 2-mercaptoethanol, and 0.1% glycerol), size-fractionated by SDS/PAGE, transferred to PVDF. Antibodies against PI3K (AF5112), Tubulin α (AF0524), antibody Bcl-2, antibodies ERK, JNK, DR5 (bs-1696R) antibody, antibody against β-actin (CST, 1:5,000), and horseradish peroxidase-conjugated antibodies against rabbit or mouse IgG were obtained. The protein bands were visualized using a Super Signal West Pico Kit, according to the manufacturer's instructions.

Data were expressed as the mean ± SD. Statistical analyses were performed using GraphPad Prism 6 software. Western blot and flow cytometry data were evaluated by independent-sample *t*-test comparing the means between two groups, and one-way analysis of variance (ANOVA), creating multiple comparison among three or more groups. Statistical significant was considered when p value was less than 0.05.

Results

Human MSCs from umbilical cord preserved the spindle-like shape typical for MSCs (Figure 1A). To further characterize the isolated hUCMSCs, they were cultured in the adipogenic, osteogenic, and neuronal complete media. Ten days after induction, intracytoplasmic lipid droplets from the hUCMSCs as the indicator of adipogenic differentiation of MSCs were detected as bright red color by Oil-red staining (Figure 1B). In addition, osteogenic differentiation of hUCMSCs was verified as brownish orange red for extracellular calcium deposits by ALP staining (Figure 1C). Neuron differentiation was confirmed by anti-betaIII Tubulin (Figure 1D), implying that the isolated hUCMSCs in this study had stem cell potential. As shown in Figure 1E, the growth curve indicated that hUCMSCs had a strong proliferative potential. Taken together, growth curves of early passages of hUCMSCs were appropriate to use in this study.

AN3CN cells were cultured with hUCMSCs-conditioned medium (UC-CM) and the proliferation was measured by CCK-8 assay for five consecutive days. UC-CM obvious inhibited the proliferation of AN3CN cells (Figures 2A, B). The effect of inhibiting proliferation was enhanced with the increase of the induction time of the UC-CM.

Since disruption of cell cycle progression may lead to in-

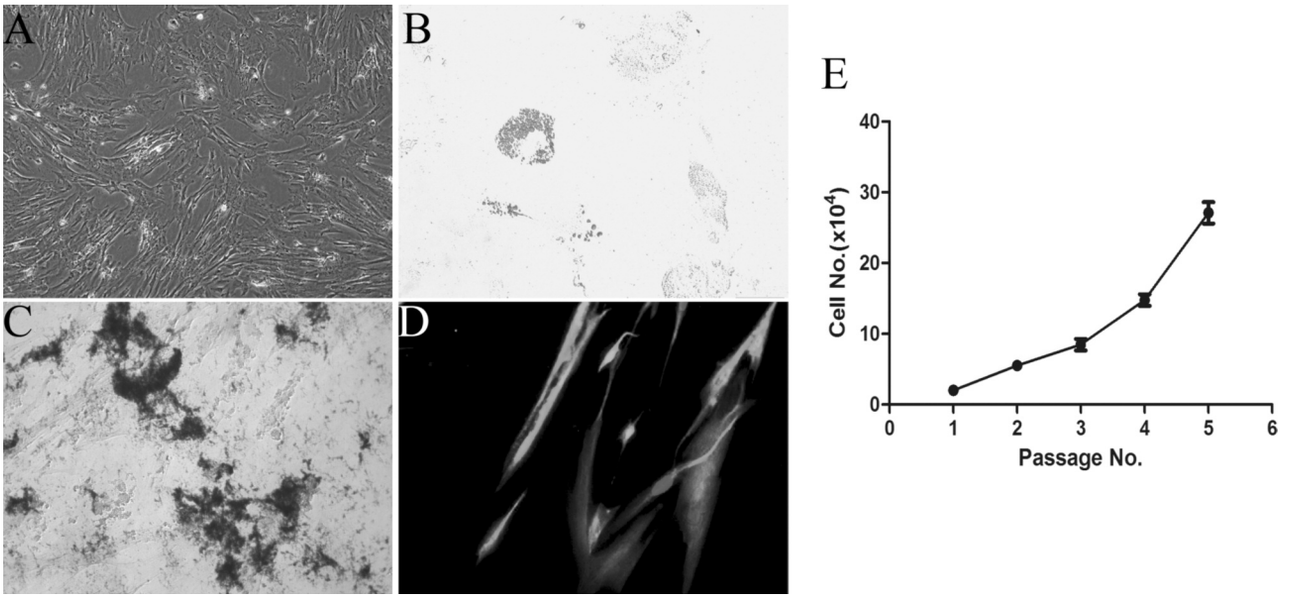

Figure 1. — Phenotypic and pluripotency of hUCMSCs. A) The isolated hUCMSCs exhibit a star-like shape with a flat morphology (magnification: ×100). B) Oil Red O staining of hUCMSCs. Intracellular lipid accumulation stained bright red in adipocytes after ten days of induction. C) Osteogenic differentiation of hUCMSCs was demonstrated by calcium deposition is detected by Gomori Alkaline Phosphatase Activity Detection Kit (HEAT). D) Neuron differentiation is determined by expressions of anti-betaIII Tubulin. E) Growth kinetics of different passages of hUCMSCs.

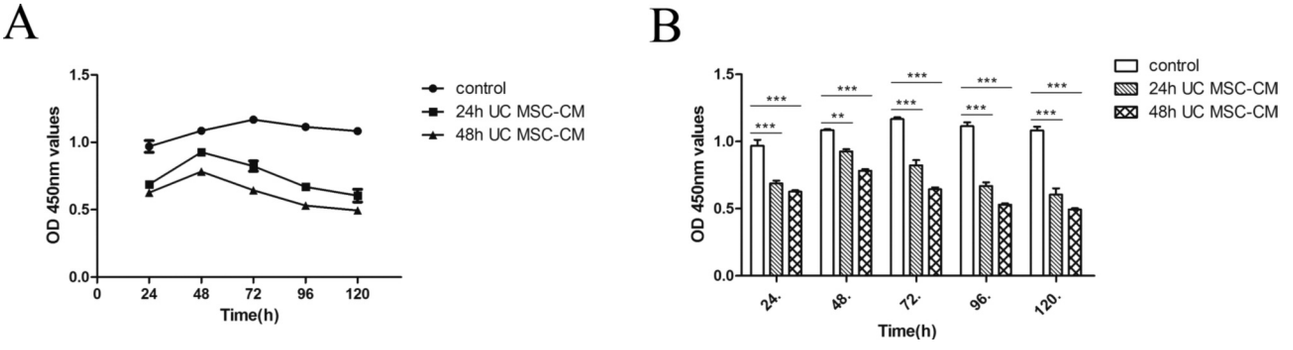

Figure 2. — The proliferation of AN3CN cells after cultured with UC-CMfor 24, 48, 72, 96, and 120 hours.

hibition of cell proliferation, the effects of MSCs-co-culture on cell cycle of AN3CN cells were investigated by flow cytometry to detect the percentage of G0/G1, S and G2/M. The fraction of G2/M phases was increased from 14.36 to 22.01% after treatment (Figure 3B), indicating that hUCMSCs conditioned medium triggered cell cycle arrest at the G2 phase.

In order to detect whether the growth inhibition of AN3CN cells by hUCMSCs was due to growth retardation or apoptosis, Annexin V-FITC/PI apoptosis assay kit was used. It showed that co-culture with hUCMSCs for 24 and 48 hours induced apoptosis of AN3CN cells with percentages of apoptosis cells increasing from 5.95% to7.83%, and 46.22%, respectively (Figure 3C).

RNA-seq technology was used to determine the changes in genes expression in AN3CN cells and AN3CN cells co-cultured with hUCMSCs (HUMIA cells). A total of 18 Gb of raw sequence data was generated from the two groups, and 2,804 genes with significantly different expression levels were identified. The transcriptome profiles of both AN3CN and HUMIA cells were compared to identify gene expression changes relating to Cell proliferation and apoptosis (Figures 4A-D).

In order to verify the transcriptome sequencing results, the expressions of specific genes were detected by Western blotting of AN3CN cells co-cultured with hUCMSCs for 24 and 48 hours. As shown in Figure 4, the expression of PI3K, Bcl-2, and α-tubulin were attenuated in co-cultured

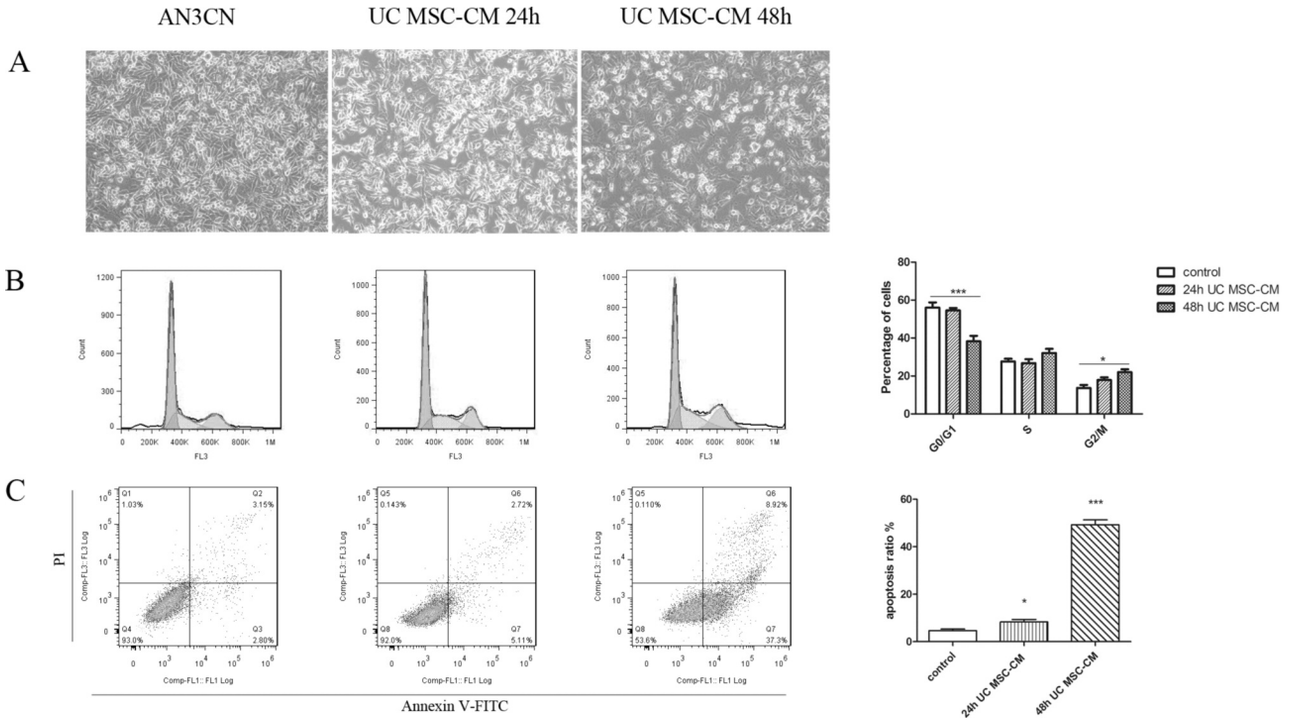

Figure 3. — Co-culture with hUCMSCs leads to cell cycle arrest and apoptosis of AN3CN. A) Morphology of AN3CN cells and cells co-cultured with hUCMSCs for 24 and 48 hours, respectively. B) Cell percentages in the G1, S, and G2/M phases of AN3CN cells co-cultured with hUCMSCs for 24 and 48 hours. C) Cell apoptosis is detected by Annexin V-FITC/PI double staining.*$p < 0.05$, ***$p < 0.001$.

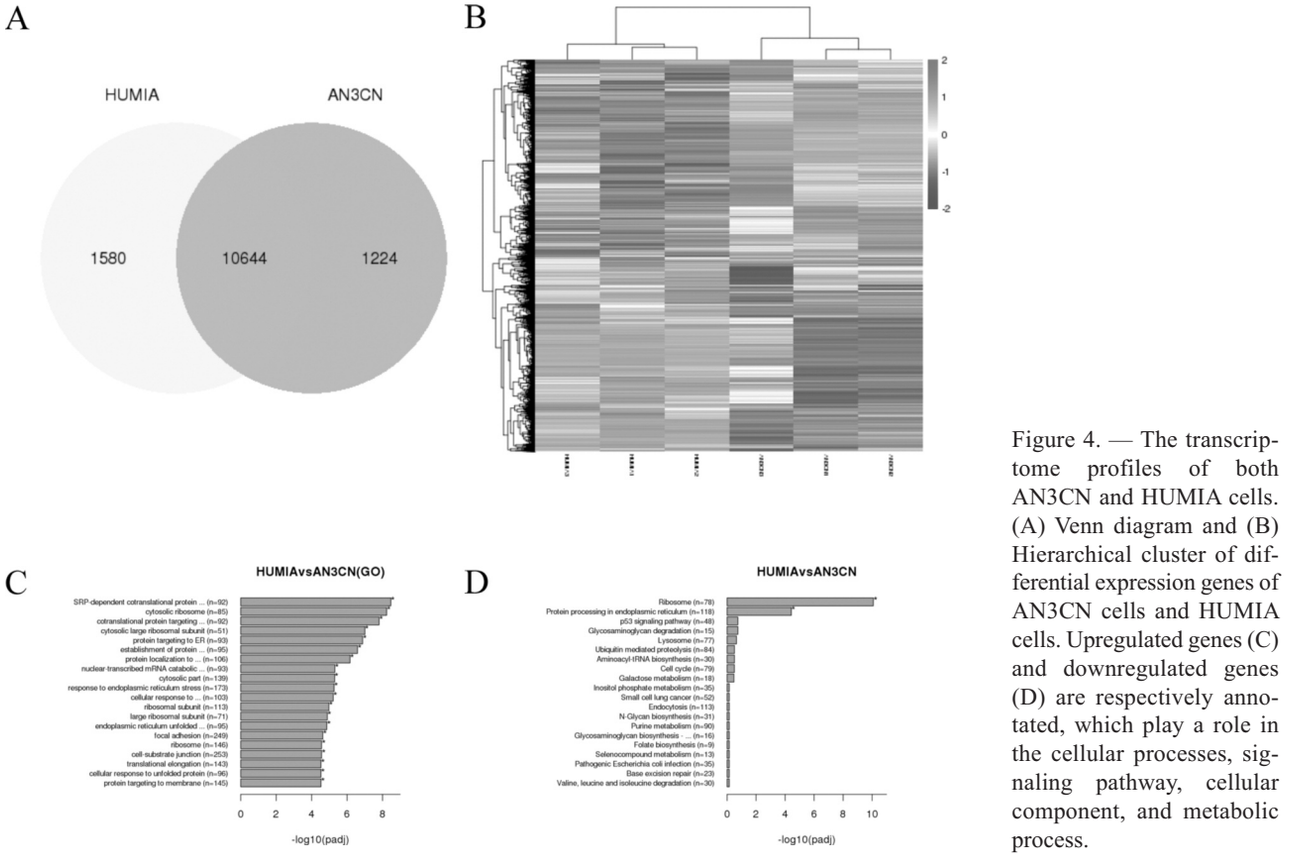

Figure 4. — The transcriptome profiles of both AN3CN and HUMIA cells. (A) Venn diagram and (B) Hierarchical cluster of differential expression genes of AN3CN cells and HUMIA cells. Upregulated genes (C) and downregulated genes (D) are respectively annotated, which play a role in the cellular processes, signaling pathway, cellular component, and metabolic process.

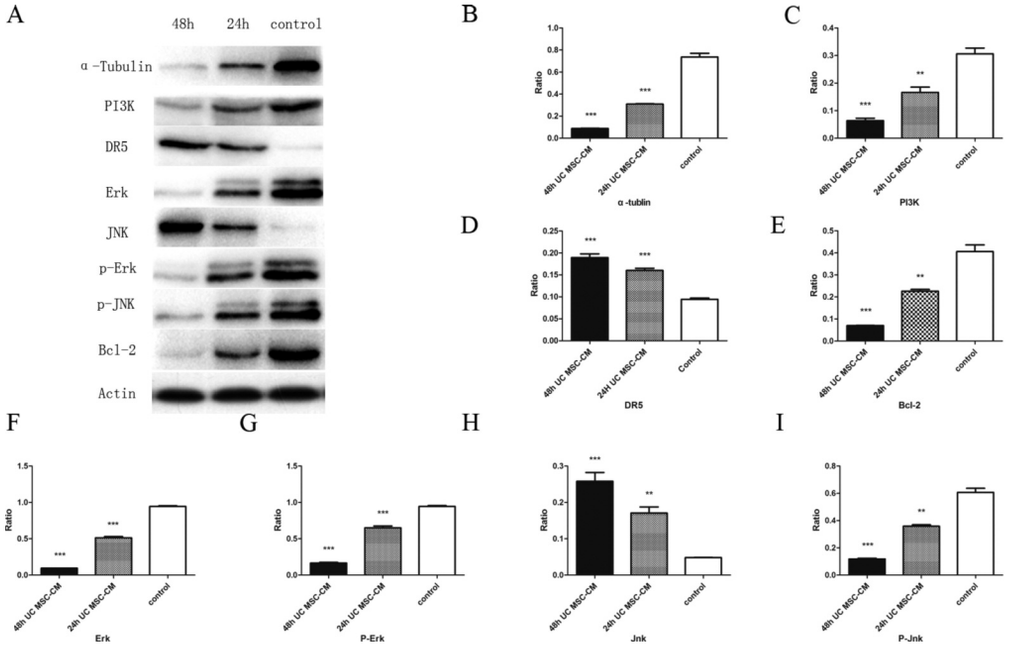

Figure 5. — The AN3CN cells are treated with hUCSCs for 24 or 48 hours, and then Western blotting is performed for analysis of protein expressions.
A) Protein expression are detected by Western blotting. B) The expression levels of protein are analyzed with ANOVA formation. $*p < 0.5$, $**p < 0.01$, and $***p < 0.001$ *vs*. control.

AN3CN cells. Furthermore, Erk, p-Erk, JNK, p-JNK, and apoptotic receptor protein DR5 were activated in AN3CN cells (Figure 5). The changes of protein levels were greater when co-culture induction time increased.

Discussion

EC is one of the most common gynecological malignancies, and its incidence is rising [14]. Recently, more attention has been paid to the interaction between hUCMSCs and tumor cells. The present authors used the hUCMSCs-conditioned medium to investigate the effect of the soluble factors from hUCMSCs on AN3CN cells. HUCMSCs treatment exhibited anti-proliferative effect on AN3CN cells, indicating that hUCMSCs targeted the growth of AN3CN cells. According to Annexin V FITC/PI staining results, co-culture with hUCMSCs induced apoptosis of AN3CN cells. The present results suggested that hUCMSCs can be a potential therapeutic approach for the treatment of cancer. This study provides the transcriptome of AN3CN cells induced by co-culture with hUCMSCs for 48 hours. Sequencing results showed that thousands of genes were differentially expressed, including ribosome-associated, endoplasmic reticulum-dependent, phagocytosis-related, and p53-related genes. In the present current research, the authors focused on the differences in gene expressions associated with apoptosis and the signaling pathways involved.

Endometrial tumors has been connected with alteration of several genes in several gene pathways. The PI3K/AKT signaling pathway is a major survival pathway in mammal cells [15]. It has critical functions in the transduction of extracellular and intracellular signals that regulates cell growth, proliferation, survival, and angiogenesis [16-18]. PI3K gene amplification was found to correlate with a PI3K activation profile which segregated more frequently to a group of aggressive and invasive tumors, notably in some groups of endometrial cancer. In the present study, the authors first detected the downregulation of PI3K gene expression in AN3CN cells co-cultured with hUCMSCs. At the same time, they also demonstrated that the expression of PI3K at the protein level was significantly reduced. It implied that the low expression of PI3K can restrain the malignant progression through inhibiting the proliferation of tumor cells and promoting the apoptosis of tumor cells of endometrial carcinoma. Inhibition of the PI3K/AKT signaling pathway might promise a novel effective approach for targeted therapy for EC in the future.

The signaling cascades associated with MAPK family include ERK and JNK, are involved in the regulation of gene expression in response to the extracellular stimulation signals and activation of various cell responses, such as cell proliferation, cell survival, cell cycle arrest, and apoptosis [19, 20]. The stimulation of a cellular death signal has been implicated with prolonged activation of phosphorylated ERK kinase [20]. The present sequencing results showed that the phosphorylation of JNK signal was upregulated in AN3CN cells co-cultured with hUCMSCs. Next, the authors verified that the phosphorylation of JNK and ERK in induced AN3CN cells was increased by Western blotting. It has been reported that JNK involved in inhibition of cell proliferation [21]. In addition, the present finding was supported by reports showing that JNK were activated in

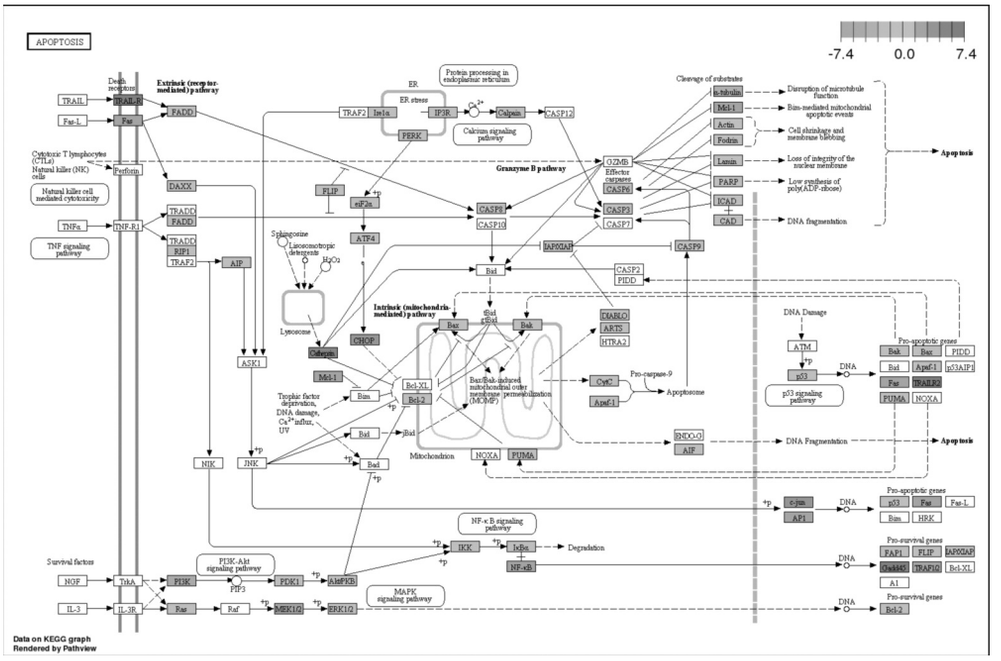

Figure 6. — The KEGG cell-cycle pathway and involving apoptosis associated gene expression. According to KEGG database, there are 12 upregulated genes (i.e.TRAIL-R, Fas, Cathepsin, CHOP, Mcl-1, MEK1/2, NF-κB, TRAILR2, c-jun, AP1, TRAF1/2, and Gadd45) and seven downregulated genes (i.e. Bcl-2, ARTS, FAP1, α-tubulin, FADD, RIP1, and PI3K) involved in apoptosis pathway. All these genes play important roles associated with apoptosis.

human cervical cancer cells [22]. Although ERK is known to function as a survival mediator in many cell types, the induction of cell death can be mediated via the activation of ERK [23, 24]. The duration of ERK activation is an important fact for determining cellular signaling, and also seems to lead to cell death [25]. In this study, JNK and ERK protein expression were significantly increased in AN3CN cells after induced by hUCMSCs.

The intrinsic pathway of cell death in cells is the mitochondria-initiated pathway. Mitochondria-dependent apoptosis is regulated by a group of proteins belonging to the Bcl-2 family [26]. Studies have shown that the high expression of anti-apoptotic Bcl-2 proteins preserves the integrity of the mitochondrial outer membrane [27]. In line with a previous authors' study, the results demonstrated a statistically significant decrease in the expression of Bcl-2 in AN3CN cells treated with hUCMSCs compared to the untreated cells. This indicated induction of AN3CN cell apoptosis through the mitochondria-mediated pathway by downregulation the expression of Bcl-2.

The internal organization, shape, polarity, motility, cell division, intracellular transport, cell differentiation, and life cycle of eukaryotic cells are all controlled by the cytoskeleton [28]. Microtubules are the largest filamentous components of the eukaryotic cytoskeleton, including actin filaments, intermediate filaments, and microtubules [29]. The microtubule is an evolutional conservative cell skeleton composed of α-tubulin and β-tubulin [30]. The present results showed that the expression of α-tubulin in AN3CN cells was significantly downregulated after induction, which could disrupt microtubule formation and consequently result in apoptosis.

Apoptosis is a type of programmed cell death, which can be induced by various stimuli either through the extrinsic or intrinsic apoptotic pathway [31]. Tumor necrosis factor-related apoptosis-inducing ligand (TRAIL) binds to its death receptor DR5 via their intracellular death domain [32]. The increased expression levels of DR5 may have enhanced the apoptotic signals in response to the increased TRAIL expression induced by the hUCMSCs. The data indicated that hUCMSCs mainly induced AN3CN cells apoptosis through a TRAIL-mediated apoptotic signaling pathway in a paracrine fashion.

In conclusion, the present results demonstrated that interactions between endometrial carcinoma AN3CN cells and hUCMSCs produced inhibitory effects on tumor cell growth and promoted apoptosis. The possible mechanisms of the apoptotic pathway are collated in Figure 6. The present research provided the potential of hUCMSCs as a new direction for the treatment of endometrial cancer. The detailed molecular pathway involved in this mechanism should be further investigated.

Acknowledgements

This study was supported by the National Natural Science Fund (Grant No. 81672583) in China.

References

[1] Chen W., Zheng R., Baade P.D., Zhang S., Zeng H., Bray F. *et al.*: "Cancer statistics in China, 2015". *CA Cancer J. Clin.*, 2016, *66*, 115.

[2] Siegel R.L., Miller K.D., Jemal A.: "Cancer statistics, 2016". CA. *Cancer J. Clin.*, 2016, *66*, 7.

[3] Rhee K.J., Lee J.I., Eom Y.W.: "Mesenchymal Stem Cell-Mediated Effects of Tumor Support or Suppression". *Int. J. Mol. Sci.*, 2015, *16*, 30015.
[4] Bexell D., Scheding S., Bengzon J.: "Toward brain tumor gene therapy using multipotent mesenchymal stromal cell vectors". *Mol. Ther.*, 2010, *18*, 1067.
[5] Bajetto A., Pattarozzi A., Corsaro A., Barbieri F., Daga A., Bosio A. *et al.*: "Different Effects of Human Umbilical Cord Mesenchymal Stem Cells on Glioblastoma Stem Cells by Direct Cell Interaction or Via Released Soluble Factors". *Front. Cell. Neurosci.*, 2017, *11*, 312.
[6] Studeny M., Marini F.C., Dembinski J.L., Zompetta C., Cabreira-Hansen M., Bekele B.N. *et al.*: "Mesenchymal stem cells: potential precursors for tumor stroma and targeted-delivery vehicles for anticancer agents". *J. Natl. Cancer Inst.*, 2004, *96*, 1593.
[7] Kidd S., Spaeth E., Dembinski J.L., Dietrich M., Watson K., Klopp A. *et al.*: "Direct evidence of mesenchymal stem cell tropism for tumor and wounding microenvironments using in vivo bioluminescent imaging". *Stem Cells*, 2009, *27*, 2614.
[8] La Rocca G., Anzalone R., Corrao S., Magno F., Loria T., Lo Iacono M. *et al.*: "Isolation and characterization of Oct-4+/HLA-G+ mesenchymal stem cells from human umbilical cord matrix: differentiation potential and detection of new markers". *Histochem. Cell. Biol.*, 2009, *131*, 267.
[9] Si Y.L., Zhao Y.L., Hao H.J., Fu X.B., Han W.D.: "MSCs: Biological characteristics, clinical applications and their outstanding concerns". *Ageing. Res. Rev.*, 2011, *10*, 93.
[10] Baraniak P.R., McDevitt T.C.: "Stem cell paracrine actions and tissue regeneration". *Regen. Med.*, 2010, *5*, 121.
[11] Ciavarella S., Caselli A., Tamma A.V., Savonarola A., Loverro G., Paganelli R. *et al.*: "A peculiar molecular profile of umbilical cord-mesenchymal stromal cells drives their inhibitory effects on multiple myeloma cell growth and tumor progression". *Stem Cells Dev.*, 2015, *24*, 1457.
[12] Bieback K., Kern S., Kluter H., Eichler H.: "Critical parameters for the isolation of mesenchymal stem cells from umbilical cord blood". *Stem Cells*, 2004, *22*, 625.
[13] Wang Y., Gao C., Zhang Y., Gao J., Teng F., Tian W. *et al.*: "Visfatin stimulates endometrial cancer cell proliferation via activation of PI3K/Akt and MAPK/ERK1/2 signalling pathways". *Gynecol. Oncol.*, 2016, *143*, 168.
[14] Siegel R., Desantis C., Jemal A.: "Colorectal cancer statistics, 2014". *CA Cancer J. Clin.*, 2014, *64*, 104.
[15] Husseinzadeh N., Husseinzadeh H.D.: "mTOR inhibitors and their clinical application in cervical, endometrial and ovarian cancers: a critical review". *Gynecol. Oncol.*, 2014, *133*, 375.
[16] Sadeghi N., Gerber D.E.: "Targeting the PI3K pathway for cancer therapy". *Future Med. Chem.*, 2012, *4*, 1153.
[17] Bauer T.M., Patel M.R., Infante J.R.: "Targeting PI3 kinase in cancer". *Pharmacol. Ther.*, 2015, *146*, 53.
[18] de Melo A.C., Paulino E., Garces A.H.: "A Review of mTOR Pathway Inhibitors in Gynecologic Cancer". *Oxid. Med. Cell. Longev.*, 2017, *2017*, 4809751.
[19] Amran D., Sanchez Y., Fernandez C., Ramos A.M., de Blas E., Breard J. *et al.*: "Arsenic trioxide sensitizes promonocytic leukemia cells to TNFalpha-induced apoptosis via p38-MAPK-regulated activation of both receptor-mediated and mitochondrial pathways". *Biochim. Biophys. Acta*, 2007, *1773*, 1653.
[20] Kim J.Y., Lee S.G., Chung J.Y., Kim Y.J., Park J.E., Koh H. *et al.*: "Ellipticine induces apoptosis in human endometrial cancer cells: the potential involvement of reactive oxygen species and mitogen-activated protein kinases". *Toxicology*, 2011, *289*, 91.
[21] Yamauchi J., Itoh H., Shinoura H., Miyamoto Y., Hirasawa A., Kaziro Y. *et al.*: "Involvement of c-Jun N-terminal kinase and p38 mitogen-activated protein kinase in alpha1B-adrenergic receptor/Galphaq-induced inhibition of cell proliferation". *Biochem. Biophys. Res. Commun.*, 2001, *281*, 1019.
[22] Kang Y.H., Lee S.J.: "The role of p38 MAPK and JNK in Arsenic trioxide-induced mitochondrial cell death in human cervical cancer cells". *J. Cell. Physiol.*, 2008, *217*, 23.
[23] Jeon E.S., Lee M.J., Sung S.M., Kim J.H.: "Sphingosylphosphorylcholine induces apoptosis of endothelial cells through reactive oxygen species-mediated activation of ERK". *J. Cell. Biochem.*, 2007, *100*, 1536.
[24] Shin G.C., Kim C., Lee J.M., Cho W.S., Lee S.G., Jeong M. *et al.*: "Apigenin-induced apoptosis is mediated by reactive oxygen species and activation of ERK1/2 in rheumatoid fibroblast-like synoviocytes". *Chem. Biol. Interact.*, 2009, *182*, 29.
[25] Murphy L.O., Blenis J.: "MAPK signal specificity: the right place at the right time". Trends. Biochem. Sci., 2006, 31, 268-275.
[26] Yang H., Yang R., Liu H., Ren Z., Wang C., Li D. *et al.*: "Knockdown of peroxisome proliferator-activated receptor gamma coactivator-1 alpha increased apoptosis of human endometrial cancer HEC-1A cells". *Onco. Targets. Ther.*, 2016, *9*, 5329.
[27] Nikolic I., Kastratovic T., Zelen I., Zivanovic A., Arsenijevic S., Mitrovic M.: "Cytosolic pro-apoptotic SPIKE induces mitochondrial apoptosis in cancer". *Biochem. Biophys. Res. Commun.*, 2010, *395*, 225.
[28] Janke C., Bulinski J.C.: "Post-translational regulation of the microtubule cytoskeleton: mechanisms and functions". *Nat. Rev. Mol. Cell. Biol.*, 2011, *12*, 773.
[29] Magiera M.M., Janke C.: "Post-translational modifications of tubulin". *Curr. Biol.*, 2014, *24*, R351.
[30] Park I.Y., Chowdhury P., Tripathi D.N., Powell R.T., Dere R., Terzo E.A. *et al.*: "Methylated alpha-tubulin antibodies recognize a new microtubule modification on mitotic microtubules". *MAbs.*, 2016, *8*, 1590.
[31] Tanaka T., Bai T., Yukawa K.: "Suppressed protein expression of the death-associated protein kinase enhances 5-fluorouracil-sensitivity but not etoposide-sensitivity in human endometrial adenocarcinoma cells". *Oncol. Rep.*, 2010, *24*, 1401.
[32] Wang S., El-Deiry W.S.: "TRAIL and apoptosis induction by TNF-family death receptors". *Oncogene*, 2003, *22*, 8628.

Corresponding Author:
BILIANG CHEN, M.D.
Department of Gynecology and Obstetrics
Xijing Hospital, The Fourth Military Medical University
15 Changle West Road
Xi'an, Shaanxi, 710032, (China)
e-mail: chenbiliang1962@sina.com